

NIST Special Publication 1200-30

Correlating mechanical abrasion with power input

Version 1.0

K. C. Scott
M. R. Wiesner
J. M. Sipe
N. Bossa

This publication is available free of charge from:
<https://doi.org/10.6028/NIST.SP.1200-30>



NIST Special Publication 1200-30

Correlating mechanical abrasion with power input

Version 1.0

K. C. Scott, 0000-0003-1022-4158
*National Institute of Standards and Technology
Material Measurement Laboratory
Gaithersburg, MD 20899-8520*

M. R. Wiesner, 0000-0002-0823-5045
J. M. Sipe, 0000-0001-5602-0922
N. Bossa, 0000-0002-5355-2744
*Duke University
Department of Civil and Environmental Engineering
Durham, NC 27708*

This publication is available free of charge from:
<https://doi.org/10.6028/NIST.SP.1200-30>

April 2022



U.S. Department of Commerce
Gina M. Raimondo, Secretary

National Institute of Standards and Technology
*James K. Olthoff, Performing the Non-Exclusive Functions and Duties of the Under Secretary of Commerce
for Standards and Technology & Director, National Institute of Standards and Technology*

Certain commercial entities, equipment, or materials may be identified in this document to describe an experimental procedure or concept adequately. Such identification is not intended to imply recommendation or endorsement by the National Institute of Standards and Technology, nor is it intended to imply that the entities, materials, or equipment are necessarily the best available for the purpose.

Publications in the SP 1200 subseries include written procedural methods in the design and implementation of experiments that ensure successful replication of results by others. Publications may include detailed procedures, lists of required equipment and instruments, information on safety precautions, the calculation of results and reporting standards.

National Institute of Standards and Technology Special Publication 1200-30
Natl. Inst. Stand. Technol. Spec. Publ. 1200-30, 13 pages (April 2022)
CODEN: NSPUE2

This publication is available free of charge from:
<https://doi.org/10.6028/NIST.SP.1200-30>

Foreword

This special publication is one in a series of protocols resulting from a collaborative research agreement between the National Institute of Standards and Technology (NIST) and Duke University's Center for the Environmental Implications of Nanotechnology (CEINT). Updates to this protocol may be released in the future. Visit <https://www.nist.gov/mml/nano-measurement-protocols> to check for revisions of this protocol or new protocols in the series.

NIST and CEINT are interested in soliciting feedback on this method. We value user comments and suggestions to improve or further validate this protocol. Please send your name, email address and comments/suggestions to nanoprotocols@nist.gov. We also encourage users to report citations to published work in which this protocol has been applied.

Key words

Abrasion; Consumer product; Manufactured nanomaterial (MNM); Microplastic (MP); Nanorelease; Nanoplastic (NP)

1. Introduction

Although there has been a significant effort to understand the mechanisms and impact of abrasion of consumer products, there are challenges in correlating results that are translatable from the laboratory to human-use or environmental phases. The abrasion rate on composite products and the effect of manufactured nanomaterials (MNMs) on these rates have been the subject of several studies [1-5]. Additionally, the generation of microplastics (MPs) from the abrasion of polymer products as a research topic is rapidly gaining in importance. Ideally, such abrasion data can be combined with power input to predict mass released during various stages of a product's life cycle. A reproducible protocol for measuring an abrasion rate that can be correlated to a specific power input is important in obtaining accurate, quantifiable, and translatable results for abrasion. To address these issues, the National Institute of Standards and Technology (NIST) and the Center for the Environmental Implications of Nanotechnology (CEINT) have developed a new abrasion apparatus and a protocol for the abrasion of grade polymer composites (both with and without MNMs) and production of MPs in testing applications.

2. Principles and scope

This Special Publication is intended to provide guidance in fabrication, operation, and data analysis of an abrasion apparatus with the ability to measure input power and the analysis of the resulting data to correlate the power dependent abrasion rate. This protocol will use nanocomposites as an example when using the machine. For more in-depth discussions of specific parameters addressed in this protocol, readers are advised to consult references Bossa et al., 2021 (for nanocomposites) and Sipe et al., 2022 (for MPs) [6-7].

3. Description of the abrasion apparatus

To simulate mechanical stress, a custom abrasion apparatus is used. The schematic diagram and a photo of the apparatus are shown in Fig. 1. The major components of the apparatus are:

- 1) air-tight abrasion chamber (30 cm by 30 cm by 30 cm) with aluminum support frame and clear polycarbonate sides;
- 2) adjustable vertical load using a combination of weights ranging from 0.05 kg to 2 kg;
- 3) holder for flat disc shaped samples;
- 4) orbital abrader with adhesive backed sandpaper or abradant;
- 5) torque meter (Datum M425¹);
- 6) stepper motor (120 V NEMA 34, 4 A, 248.7 W (1/3 hp), 361 rad/s (3450 RPM));
- 7) inlet and outlet (sampling) ports; and
- 8) displacement measurement using linear variable differential transformer (LVDT) sensor.

¹ Certain commercial entities, equipment, or materials may be identified in this document to describe an experimental procedure or concept adequately. Such identification is not intended to imply recommendation or endorsement by the National Institute of Standards and Technology, nor is it intended to imply that the entities, materials, or equipment are necessarily the best available for the purpose.

The apparatus is designed to abrade the surface of a disc shaped sample by pressing the sample onto an orbital abrader (e.g., sandpaper) head as in typical sanding applications. For a similar sandpaper, the effective coefficient of friction can be adjusted by changing the vertical load (i.e., weights placed on the apparatus). The sample holder and the abrader head are enclosed in an airtight chamber. The inlet ports can be used to introduce cooling water or gas to prevent overheating and melting of the samples during the abrasion process. The outlet/sampling port can be used to collect aerosol and MPs produced during the abrasion process for subsequent characterization and analyses.

This apparatus incorporates a torque meter (Newton meter (Nm)) to measure the time dependent energy input into the abrasion process. During an abrasion process, the release rate of particles is dependent on the input energy (Joules (J)) which is directly proportional to tangential force (Newtons (N)), i.e., friction force, and sliding distance (meters (m)). The amount of force put on the sample is controlled using a combination of load weights ranging from 0.1 kg to 2 kg.

The abrading apparatus also can be used with a highly sensitive linear variable differential transformer (LVDT) to measure material loss in real time rather than taking the mass difference of the sample before and after testing.

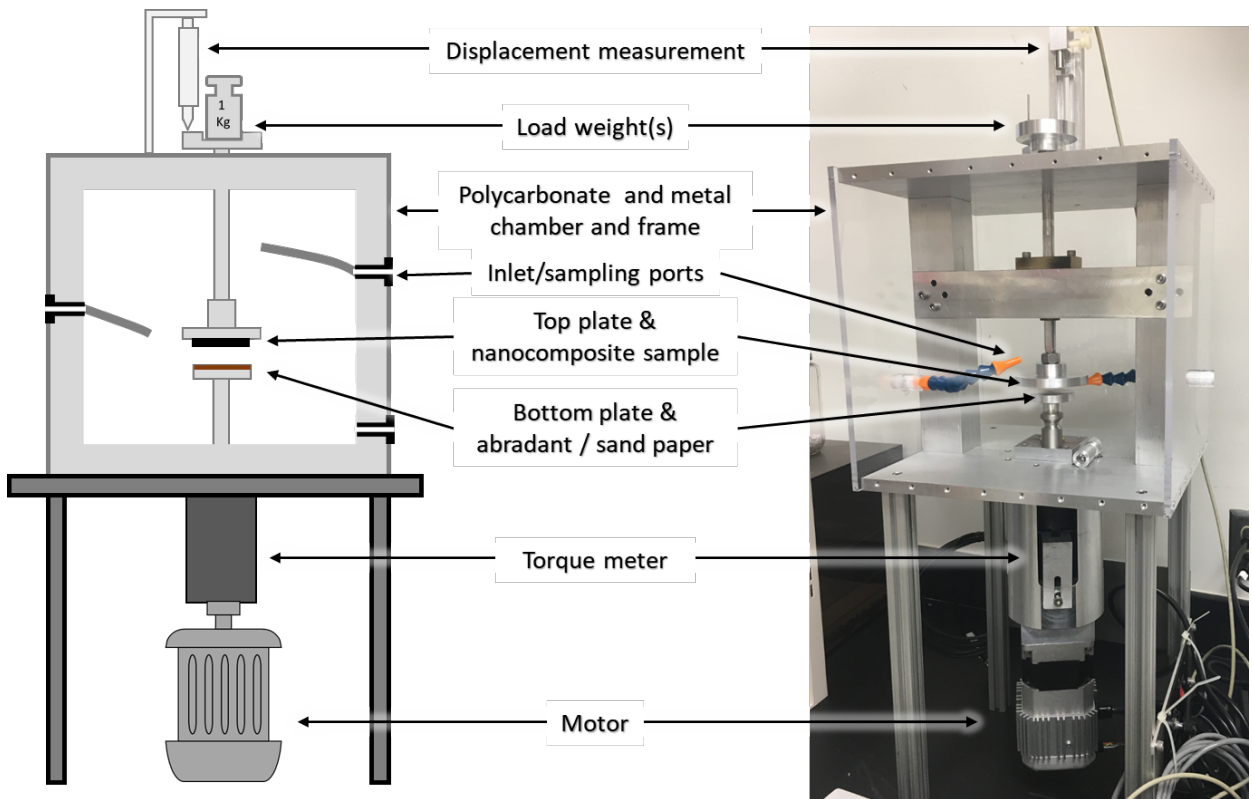


Fig. 1. Overview of the abrasion apparatus

4. Materials, equipment, and apparatus

4.1. Materials

- Test sample, 5 cm diameter x 5 mm thick, neat polymer or nanocomposite disc.
- 100 grit aluminum oxide sandpaper with adhesive backing, 5 cm (2 inch) diameter.
- Adhesive (double sided tape and/or glue) for attaching the test sample to the sample holder.
- Clean piece of paper for collecting abraded particles. Kitchen parchment paper works well.

4.2. Equipment and apparatus

- Laboratory balance with 0.001 g or better (< 0.001 g) readability.
- Abrasion apparatus described in Section 3.
- Data acquisition and analysis computer, connected to the torque meter on the abrasion apparatus.
- Stopwatch.

4.3. Pre-requisite data

- Mass of the load assembly. The total load during abrasion is the sum of the added mass, load assembly mass, top plate and sample assembly mass.

5. Abrasion experiment

1. Before each experimental run, open the abrasion chamber and clean the inside by wiping down the chamber walls and surfaces. Make sure that the detached panel is cleaned also.
2. Place the desired weight on top. Record the mass of the added weight.
3. If collecting particles (e.g., MPs), place a piece of clean parchment paper to cover the bottom of the chamber. Make sure that the entire bottom surface is covered. Cut out a hole in the middle to accommodate the rotating pole.
4. Affix the sandpaper to the lower plate.
5. Attach the bottom plate to the abrasion apparatus.
6. Attach the test sample to the top plate using adhesives.
7. Weigh the top plate and test sample assembly. Record the mass.
8. Attach the top plate with the test sample to the abrasion apparatus.
9. Seal the abrasion chamber.
10. Turn on the torque meter and zero the torque meter.
11. Power on the motor and set the motor speed (e.g., 62.8 rad/s (600 RPM) or 157 rad/s (1500 RPM))
12. Once the desired motor speed is reached, run for additional 1 minute then stop the torque data collection.
13. Turn off the motor.
14. Open the chamber.
15. Remove the top plate and test sample assembly and weigh the assembly.
16. Re-attach the top assembly to the apparatus.
17. Close the chamber.
18. Repeat steps 10 through 15 as needed. The total repeat number will depend on the number of replicates and experimental setting levels (e.g., n motor speed levels, m load weight levels, etc.) used.

19. To process another sample, remove the abraded test sample from the top plate and the used sandpaper from the bottom plate.

For each test, the sample disc is abraded at a specific speed and run for a specific duration, with the top plate and product being removed after each increment and re-weighed. The abradant is changed after every test to ensure that it is not too worn down. Table 1 shows a typical test and run parameters.

Table 1. Example test and run parameter matrix.

| Test Material | TEST # | RUN # | Motor Speed (rad/s) | Abrasion Duration (min) | Load Weight (kg) |
|---------------|--------|-----------------|---------------------|-------------------------|------------------|
| Neat polymer | 1 | Run 1 | 62.8 | 1 | 0.2 |
| | | Run 1 Replicate | 62.8 | 1 | 0.2 |
| | | Run 2 | 62.8 | 1 | 0.5 |
| | | Run 2 Replicate | 62.8 | 1 | 0.5 |
| | | Run 3 | 62.8 | 1 | 1 |
| | | Run 3 Replicate | 62.8 | 1 | 1 |
| | | Run 4 | 62.8 | 1 | 2 |
| | | Run 4 Replicate | 62.8 | 1 | 2 |
| | 2 | Run 1 | 157 | 1 | 0.2 |
| | | Run 1 Replicate | 157 | 1 | 0.2 |
| | | ⋮ | | | |
| Nanocomposite | 1 | Run 1 | 62.8 | 1 | 0.2 |
| | | ⋮ | | | |

6. Data analysis

6.1. Power dependent abrasion quantification

Taber abrader which was originally designed for textile wear testing is a commonly used abrasion device. For microplastics research, cryomills are often used to generate micro-sized plastic particles from bulk plastic components. However, methods have not been developed for either instrument to successfully estimated the rate of abrasion nor do they provide a basis for extrapolating abrasion rates from laboratory to other systems. The power input, time, and surface area of the material in a given abrasion scenario are needed to calculate the rate of micro- and nano-plastic production. These input power dependent abrasion rates can be used for hazard and risk analysis on limits of exposure and provide input values for modeling mechanical breakdown of products during use and in the environment.

This abrasion apparatus described here uses a torque meter attached to the motor to measure the force applied on the sample during abrasion. This torque measurement combined with the

gravitational force from the top weight contributes to the input energy value. This input energy along with the mass lost during abrasion allow us to make a per unit mass energy rate that can be compared between different material samples.

The power input for a given abrasion scenario is calculated using Eqn. 1 where power P (J/s) is related to torque T (N·m) by the angular velocity ω (rad/s):

$$P = \omega \times T \tag{Eq. (1)}$$

The abrasion rate ($\text{g}/(\text{s}\cdot\text{m}^2)$) can be calculated using Eqn. 2 where m_1 (g) and m_2 (g) are the before and after run sample masses, respectively, t (s) is the duration of the abrasion run and r (m) is the radius of the disc sample:

$$\text{abrasion rate} = \frac{\pi r^2(m_1 - m_2)}{t} \tag{Eq. (2)}$$

Each abrasion run generates one data point on the abrasion rates vs. power plot. Abrasion rate as a function of input power for a specific sample material can be plotted using these data points. For more detailed discussion of the data analysis and theory, refer to Bossa et al. [6].

6.2. Worked example

A typical output file from a torque meter should contain date and timestamp, measured torque, measured rotational speed, and calculated power as shown in Fig. 2. Make sure that the motor speed has stabilized before starting the run timer.

| Date | Time | Torque(Nm) | Speed | Watts |
|-----------|----------|------------|----------|--------|
| 14-7-2021 | 14:59:53 | -0.010 | 0.000 | 0.000 |
| 14-7-2021 | 14:59:53 | 0.000 | 0.000 | 0.000 |
| 14-7-2021 | 14:59:53 | -0.010 | 0.000 | 0.000 |
| 14-7-2021 | 14:59:53 | 0.010 | 0.000 | 0.000 |
| 14-7-2021 | 14:59:53 | 0.000 | 0.000 | 0.000 |
| 14-7-2021 | 14:59:53 | 0.000 | 0.000 | 0.000 |
| 14-7-2021 | 14:59:56 | 0.110 | 1091.000 | 12.567 |
| 14-7-2021 | 14:59:56 | 0.100 | 1108.000 | 11.603 |
| 14-7-2021 | 14:59:57 | 0.090 | 1108.000 | 10.443 |
| 14-7-2021 | 14:59:57 | 0.110 | 1111.000 | 12.798 |
| 14-7-2021 | 14:59:57 | 0.100 | 1127.000 | 11.802 |
| 14-7-2021 | 14:59:57 | 0.100 | 1127.000 | 11.802 |
| 14-7-2021 | 14:59:58 | 0.100 | 1123.000 | 11.760 |
| 14-7-2021 | 14:59:58 | 0.110 | 1113.000 | 12.821 |
| 14-7-2021 | 14:59:58 | 0.090 | 1113.000 | 10.490 |
| 14-7-2021 | 14:59:58 | 0.100 | 1107.000 | 10.433 |
| 14-7-2021 | 14:59:58 | 0.100 | 1100.000 | 11.519 |
| 14-7-2021 | 14:59:59 | 0.090 | 1100.000 | 10.367 |

Fig. 2. Output file from torque meter

Table 2 shows typical data table columns for a material. Once all the runs are completed, plot the (power, abrasion rate) data points for each material and fit a line passing through the origin that best fit the data. The y-intercept should be 0 since there can be no negative abrasion. From this line of best fit, a p-value on the x and y variables and standard error on the slope of the line of best fit is determined. An example plot is shown in Sec. 7, Fig. 3.

Table 2. Typical experimental data table columns

| Data Column | Description |
|-------------------------------------|---|
| Sample ID | |
| Sample Material | Type of material that is being tested |
| Abrasive Material | Abradant details, material, size |
| Sample Type | Shape, source, use, etc. |
| Surface Area (m ²) | Surface area that is in contact with the abrasive material during abrasion |
| Load Mass (kg) | Mass that was placed on top of the abrasion machine during the specific run |
| Run # | Run ID |
| Time (s) | Abrasion duration, Timing should start as soon as the motor speed stabilizes and motor should be stopped as soon as the desired abrasion time has been reached. |
| Speed (rad/s) | Target motor speed |
| Background Torque (Nm) | This value is usually zero, but if the torque meter is not properly zeroed before a test run this column will contain a value other than zero. |
| Average Torque (Nm) | Average torque that was calculated manually from the torque meter output file. |
| Corrected Torque (Nm) | Average torque minus background torque |
| Initial Sample Mass (g) | Sample mass before each abrasion run |
| Final Sample Mass (g) | Sample mass after each abrasion run |
| Mass Abraded (g) | Initial sample mass minus final sample mass |
| Input Power (W) | Equation 1 |
| Abrasion Rate (g/s/m ²) | Equation 2 |
| Notes | |

7. Extrapolating lab results to human or environmental implication

Various use scenarios can be compared in terms of the different power inputs creating abrasion. However, scenarios will differ not only in their instantaneous power input, but in the time that the material is exposed to that power input; for example, chewing may have high power inputs over short periods of time, while erosion from wave action may involve lower power inputs over extended periods of time. Integrating power over time yields the work done on the abraded object.

Fig. 3 shows an abrasion rate plot from Bossa et al. [6]. In this example, PETG-0, PETG-0.5, and PETG-2 refer to polyethylene terephthalate glycol composite with 0 %, 0.5 %, and 2 % by mass fraction of multiwall carbon nanotubes, respectively.

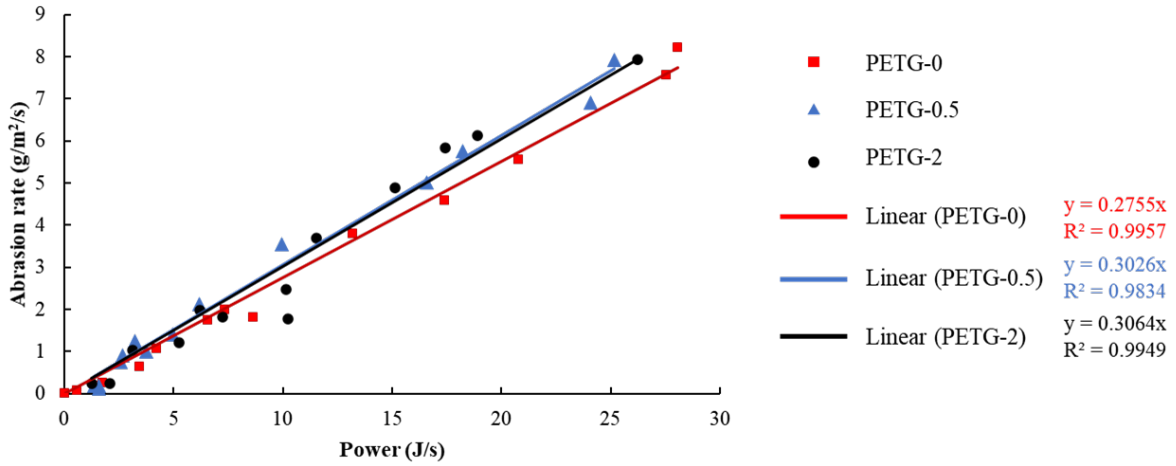


Fig. 3. Abrasion rate plot example from Bossa, et al. showing the measured and fitted abrasion rates as a function of input power for several different nanocomposites [6].

Consider the two use scenarios where abrasion of a similar plastic product occurs by sanding (ranges from 1 J/s to 300 J/s based on sander used) or chewing (average male jaw around 61 J/s) [8-11]. Abrasion rate of PETG-2 can be calculated for a specific power input (e.g., 1 J/s) value simply by multiplying the slope of the fitted line (0.3064 from Figure 3) by the power input to obtain a value for abrasion rate of 0.31 g/m²/s [9]. In this manner, abrasion rates of specific plastic materials during various use scenarios can be determined. Table 3 shows estimated abrasion rates for different PETG nanocomposites for sanding and chewing based on reported power inputs for these operations.

Table 3. Estimated abrasion rates for different abrasion scenarios based on the measured abrasion data for PETG nanocomposite in Bossa, et al. [6].

| Scenario | Power input (J/s) | Material | Abrasion rate function | Abrasion rate (g/m ² /s) |
|----------|---|----------|------------------------|-------------------------------------|
| Sanding | 1 to 300 Based on: 1-3 J/s [8] 300 J/s [9] | PETG-0 | $y = 0.2755x$ | 0.28 to 83 |
| | | PETG-0.5 | $y = 0.3026x$ | 0.3 to 90 |
| | | PETG-2 | $y = 0.3064x$ | 0.31 to 92 |
| Chewing | 61 Based on: Mean molar force for men, 383.9 N [10] Average male jaw length, 118.5 mm [11] | PETG-0 | $y = 0.2755x$ | 17 |
| | | PETG-0.5 | $y = 0.3026x$ | 18 |
| | | PETG-2 | $y = 0.3064x$ | 19 |

| | | | | |
|--|--|--|--|--|
| | $\frac{383.9 N \times 0.1185m}{0.75 s \text{ chew time}}$ $= 61 J/s$ | | | |
|--|--|--|--|--|

8. Abbreviations

| | |
|------|---|
| LVDT | Linear variable differential transformer |
| MNM | Manufactured Nanomaterials |
| MP | Microplastic |
| NEMA | National Electrical Manufacturers Association |
| PETG | Polyethylene terephthalate glycol |
| RPM | Revolutions per minute |

References

- [1] Gohler D, Stintz M, Hillemann L, Vorbau M (2010) Characterization of nanoparticle release from surface coatings by the simulation of a sanding process. *Ann. Occup. Hyg.* 54 (6), 615-24.
- [2] Koponen IK, Jensen KA, Schneider T (2011) Comparison of dust released from sanding conventional and nanoparticle-doped wall and wood coatings. *J. Expo. Sci. Environ. Epidemiol.* 21 (4), 408-18.
- [3] Gomez V, Levin M, Saber AT, Irusta S, Dal Maso M, Hanoi R, Santamaria J, Jensen KA, Wallin H, Koponen IK (2014) Comparison of dust release from epoxy and paint nanocomposites and conventional products during sanding and sawing. *Ann. Occup. Hyg.* 58 (8), 983-94.
- [4] Ding Y, Wohlleben W, Boland M, Vilsmeier K, Riediker M (2017) Nano-object Release During Machining of Polymer-Based Nanocomposites Depends on Process Factors and the Type of Nanofiller. *Ann. Work. Expo. Health* 61 (9), 1132-1144.
- [5] Wohlleben W, Meier MW, Vogel S, Landsiedel R, Cox G, Hirth S, Tomovic Z (2013) Elastic CNT-polyurethane nanocomposite: synthesis, performance and assessment of fragments released during use. *Nanoscale* 5 (1), 369-80.
- [6] Bossa N, Sipe JM, Berger W, Scott K, Kennedy A, Thomas T, Hendren CO, Wiesner MR (2021) Quantifying Mechanical Abrasion of MWCNT Nanocomposites Used in 3D Printing: Influence of CNT Content on Abrasion Products and Rate of Microplastic Production. *Environ. Sci. & Technol.* 55 (15), 10332-10342.
- [7] Sipe JM, Bossa N, Berger W, von Windheim N, Gall K, Wiesner MR (2022) From bottle to microplastics: Can we estimate how our plastic products are breaking down? *Science of The Total Environment* 814, 152460.
- [8] Luo B, Li L, Liu H, Xu M, Xing F (2014) Analysis of sanding parameters, sanding force, normal force, power consumption, and surface roughness in sanding wood-based panels. *BioResources* 9 (4), 7494-7503.
- [9] Loredana MR, Anne-Marie BL (2015) Research on Power Consumption for Sanding Process with Abrasive Brushes to Solid Spruce and MDF Panels. *Procedia Engineering* 100, 1495-1504.
- [10] Lepley CR, Throckmorton GS, Ceen RF, Buschang PH (2011) Relative contributions of occlusion, maximum bite force, and chewing cycle kinematics to masticatory performance. *American Journal of Orthodontics and Dentofacial Orthopedics* 139 (5), 606-613.
- [11] Du LL, Wang LM, Zhuang Z (2008) Measurement and analysis of human head-face dimensions. *Chinese Journal of Industrial Hygiene and Occupational Diseases* 26 (5), 266-270.